Journal of Applied Electrochemistry **32**: 505–512, 2002.

Electrochemical properties of Pb–Sb, Pb–Ca–Sn and Pb–Co_3O_4 anodes in copper electrowinning

A. HRUSSANOVA*, L. MIRKOVA and TS. DOBREV
Institute of Physical Chemistry, Bulgarian Academy of Sciences, Department 'Elchim', Acad. G. Bonchev, bl.11, 1113 Sofia, Bulgaria
*(*author for correspondence, e-mail: antoanet@ipchp.ipc.bas.bg)*

Received 3 April 2001; accepted in revised form 19 February 2002

Key words: composite Pb–Co coating, copper electrowinning, Pb–Sb anode, Pb–Sn–Ca anode

Abstract

Three types of anode, Pb–Sb, Pb–Ca–Sn and Pb–Co_3O_4, for copper electrowinning were investigated. The corrosion resistance, as evaluated by cyclic voltammetric (CV) measurements was higher for Pb–Co_3O_4 than for Pb–Sb and Pb–Ca–Sn. During prolonged electrowinning under galvanostatic conditions, the anodic reaction on the Pb–Co_3O_4 anode was depolarized by 0.053 V as compared to Pb–Sb, and by 0.106 V with respect to Pb–Ca–Sn. The composition and structure of the anodic layer were determined by XPS, X-ray and SEM analyses. The surface layer on the three anodes examined was composed mainly of $PbSO_4$, α-PbO_2 and β-PbO_2. Different structure of the surface layer was observed: loose and highly spread coral-like structure in the case of Pb–Sb; fibrous structure in the case of Pb–Ca–Sn and dense, fine-grained structure in the case of Pb–Co_3O_4.

1. Introduction

Lead, alloyed with 6–10% Sb has been widely used as anode material in copper electrowinning. In this system, Sb lowers the oxygen overvoltage on Pb. Recent studies [1] have shown that the addition of Co^{2+} to the electrolyte in a conventional cell leads to an even more pronounced decrease in oxygen overvoltage on the Pb–Sb anode as compared to the case when dimensionally stable anodes (DSA) are used. The corrosion rate of the Pb–Sb anode increases with the Sb concentration [2, 3]. It is found that the addition of Co^{2+} ions to the electrolyte significantly reduces the corrosion rate of the anode, as well as the cathode contamination with Pb [4–6]. According to Koch [7], less PbO_2 is formed on the surface of lead anodes when 200 mg l^{-1} Co^{2+} (as $CoSO_4$) are added to 1 M H_2SO_4 solution.

With the advent of solvent extraction-electrowinning for producing high purity cathode deposits, the need arises for lowering lead levels in the cathode deposit. New alloys of Pb with Ca and/or Sr were developed to reduce the rate of spalling of PbO_2 from the anode compared with the conventional Pb–Sb, and thus to decrease the Pb level in the cathode. The quantity of Ca and Sr in these alloys must be carefully controlled to produce a fine-grained structure with minimal alloy segregation [8, 9]. The Pb–Ca and Pb–Sr alloys are relatively weak and, for that reason, Sn is added to improve the mechanical properties and to decrease the creep rate. The rolled non-antimony alloys show high corrosion resistance, the effect being more evident when Co^{2+} ions are added to the electrolyte. The Pb–Ca–Sn anodes are strong, uniform, dross and crack-free, with a fine-grained structure and, moreover, they show uniform corrosion [10].

A new lead alloy with low levels of Sb and Sn has also been developed for use as anode [11, 12]. This alloy shows a uniform fine-grained structure. As the Sb content is sufficiently low, there is no interconnecting network of Sb and corrosion is reduced. There is sufficient Sb, however, to produce a nonreactive β-PbO_2 phase which prevents passivation. It combines the advantages of the older high Sb alloys and the newer non-antimonial Pb–Ca and Pb–Sr alloys.

It has been found that a minimal quantity of Co in the Pb anode significantly decreases both the rate of corrosion and the oxygen evolution overpotential [13]. Forsen et al. [14] have shown that plasma sprayed and detonation deposited Pb–Co alloy decreases the anode overpotential as in the case when Co^{2+} ions are added to the electrolyte. By means of electroforming (pulse plating), Rashkov et al. [15] have obtained thick Pb layers with Co content in the range from 0.5 to 6% (by weight). In zinc electrowinning, the same authors have shown that the corrosion rate of pulse-plated Pb–Co layers with Co content of no less than 2% is negligible, and moreover, the presence of Co leads to the formation of a dense and stable surface film. The anode overpotential of Pb–Co with a Co content of about 3% is lower than that of Pb–Ag (1%) (a classical anode,

usually used in zinc electrowinning) by 0.08–0.1 V. Two types of quaternary metallurgical alloy: Pb–Ag 0.2–Sn 0.06–Co 0.03 and Pb–Ag 0.2–Sn 0.12–Co 0.06 have been produced and compared [16]. They also show lower anodic polarization than that of the Pb–Ag anode. This effect is mainly due to the favourable effect of cobalt.

Recently, a new anodic material for metal electrowinning has been developed on the basis of a Pb–Co composite coating (with 1–3% Co) on a Pb substrate. In the case of zinc electrowinning [17], this composite anode has shown a low corrosion rate and a depolarizing effect on the anodic reaction. A comprehensive study of the behaviour of a Pb–Co_3O_4 composite anode in copper electrowinning has been recently reported [18].

This paper presents a further electrochemical study of the composite anode (Pb–Co_3O_4) in copper electrowinning by different techniques. The electrocatalytic and corrosion properties of this anode are compared with two other types of anode, widely used in industrial practice: Pb–Sb and Pb–Ca–Sn.

2. Experimental details

2.1. *Composition of the electrolyte for copper electrowinning*

The composition of the basic electrolyte (BE) for copper electrowinning was as follows:

30 g l^{-1} Cu^{2+} (0.47 M $CuSO_4 \cdot 5H_2O$) and 85 g l^{-1} (0.87 M) H_2SO_4.

2.2. *Anodes*

The following types of anode were investigated: (i) cast Pb–Sb (Sb 5.85%) metallurgical alloy; (ii) hot rolled Pb–Ca–Sn (Ca 0.081%, Sn 0.74%, Al 0.01%) metallurgical alloy, supplied from UM, Belgium; and (iii) Pb–Co_3O_4 (3% Co) coating on Pb substrate.

The bath for electrodeposition of Pb–Co_3O_4 (about 3% Co) composite coating consisted of 60 g l^{-1} Co^{2+} (as Co_3O_4 particles with a specific active surface of 16 m^2 g^{-1}); 150 g l^{-1} $Pb(NH_2SO_3)_2$; 100 g l^{-1} NH_2SO_3-NH_4; 1 g l^{-1} *o*-toluidine and 0.2 g l^{-1} glue. The Pb–Co_3O_4 coating was plated on a lead substrate at room temperature and a cathodic current density of 10 mA cm^{-2}. Pb anodes and air bubbling of the bath suspension were used. The thickness of the Pb–Co_3O_4 coatings was about 90 μm (after about 3 h deposition).

The preliminary treatment of the lead substrate included: (i) cleaning in alcohol; (ii) 5 min cathodic degreasing in a solution of 40 g l^{-1} $Na_3PO_4 \cdot 12H_2O$ under the following conditions: room temperature, cathodic current density of 50 mA cm^{-2}, stainless steel anodes; (iii) 1 min anodic etching in 10% HBF_4 solution: room temperature, anodic current density of 50 mA cm^{-2}, Pt cathodes; and (iv) final rinsing with distilled water before electrodeposition of the Pb–Co_3O_4 coating.

2.3. *Techniques*

2.3.1. *CVA method*

The cyclic voltammograms of the Pb–Sb, Pb–Ca–Sn and Pb–Co_3O_4 anodes (a geometric area of 1 cm^2) were obtained at the very beginning of galvanostatic polarization (0 h), at the 24th and 96th hour from the beginning of polarization, when the PbO_2 layer had already been formed. The anodic polarization under galvanostatic conditions was performed at 10 mA cm^{-2} in a glass cell at constant temperature of 25 °C. A copper plate of 1 cm^2 area served as cathode. The reference electrode was Hg/Hg_2SO_4 (SSE). To avoid copper deposition on the anode, potential scanning was carried out in the range −0.4 to 2.0 V vs SSE. The potential sweep rate was 10 mV s^{-1}. Taking into account that oxidation reactions of Pb to $PbSO_4$ and of $PbSO_4$ to PbO_2, as well as the corresponding reduction reactions, run through the conductive PbO_2 layer, the height of corresponding current maxima was used as a measure of the amount of $PbSO_4$ and PbO_2 in the surface film.

2.3.2. *Galvanostatic method*

Electrolysis with Pb–Sb, Pb–Ca–Sn or Pb–Co_3O_4 anode (geometric area of 1 cm^2) was performed in a glass cell at an anodic current density of 10 mA cm^{-2} and constant temperature of 25 °C. A copper plate of 1 cm^2 served as cathode. The reference electrode was Hg/Hg_2SO_4 (SSE). A millivoltmeter with a high ohmic input (5×10^{12} Ω) indicated the potential during prolonged polarization. The duration of the experiments was 360 h.

2.3.3. *XPS and X-ray analysis*

Using XPS and X-ray analysis, information about the composition of the surface layer on Pb–Sb, Pb–Ca–Sn and Pb–Co_3O_4 anodes was obtained. At the 96th hour of anodic polarization at 10 mA cm^{-2}, the samples were rinsed, dried and analysed.

XPS measurements were carried out using an Escalab Mk II (VG Scientific) electron spectrometer.

The phase composition of the anodic layer on Pb–Sb, Pb–Ca–Sn and Pb–Co_3O_4 anodes was determined by a X-ray phase analysis using a Philips APD-15 diffractometer (CuK_α radiation).

2.3.4. *SEM observation*

At the 96th hour of anodic polarization at 10 mA cm^{-2}, the surface morphology of the anodic layer on Pb–Sb, Pb–Ca–Sn and Pb–Co_3O_4 anodes was investigated using a scanning electron microscope (SEM) (Jeol-Superprobe 733). Before being analysed, the samples were rinsed and dried.

3. Results and discussion

3.1. *Anodic behaviour by cyclic voltammetry*

Figure 1 shows the cyclic voltammograms of the Pb–Sb anode at the start time, at 24th hour and 96th hour of

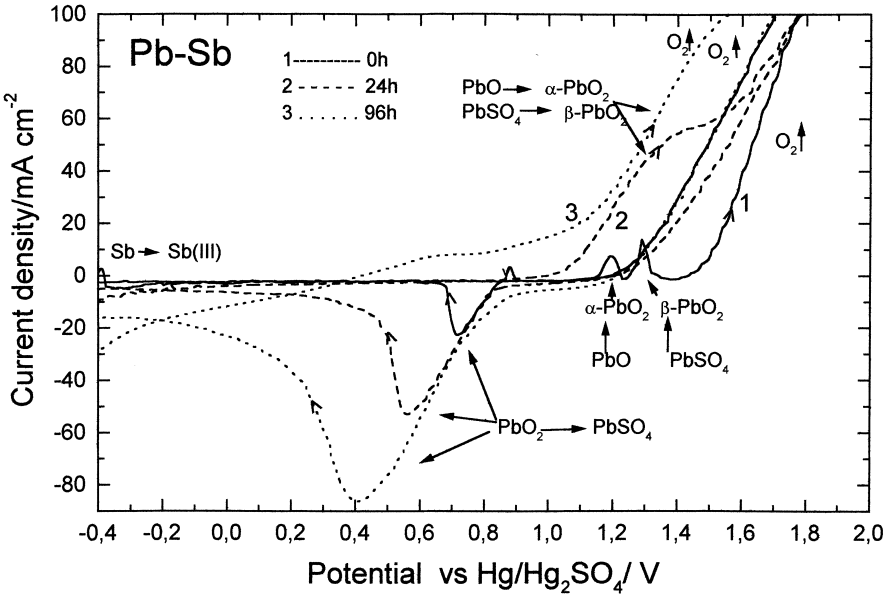

Fig. 1. Cyclic voltammograms of Pb–Sb anode obtained at the start time, at the 24th hour and at the 96th hour of the anodic polarization.

anodic polarization. The cyclic voltammogram at the start time is characterized by three anodic peaks and one anodic branch during scanning in the positive direction, and by one anodic and one cathodic peak at the negative scanning. The anodic peak, appearing at −0.4 V is due to the oxidation of Sb to Sb(III) [19, 20]. The anodic peaks at 1.2 and 1.3 V are probably due to the oxidation of PbO to α-PbO_2 and of $PbSO_4$ to β-PbO_2, respectively [21]. The sharp increase in current after 1.5 V (anodic branch) is due to oxygen evolution [21, 22]. The anodic peak at 0.85 V during scanning in the negative direction is probably due to oxidation of metallic lead and/or to incompletely oxidized products of Pb [23]. The cathodic peak at 0.7 V is due to the reduction of α- and β-PbO_2 to $PbSO_4$ [21]. The various peaks appearing about the $PbO_2/PbSO_4$ potential (0.7–0.8 V) during negative scanning are explained in detail by Sharp [24]. According to this author, these peaks are caused by the simultaneous cathodic and anodic reactions of Pb ions in the range 0.6 to 1.0 V (vs $Hg/HgSO_4$). As reported by Mahato [19], the increase in Sb content of the alloy leads to a decreased anodic peak height, following the cathodic discharge of PbO_2 during negative scanning. With a Sb content of about 6%, this anodic peak disappears. In agreement with the data of Mahato, such an anodic peak is not observed on the corresponding curve of the Pb–Sb anode. After prolonged polarization (see again Figure 1), the part of the curves corresponding to

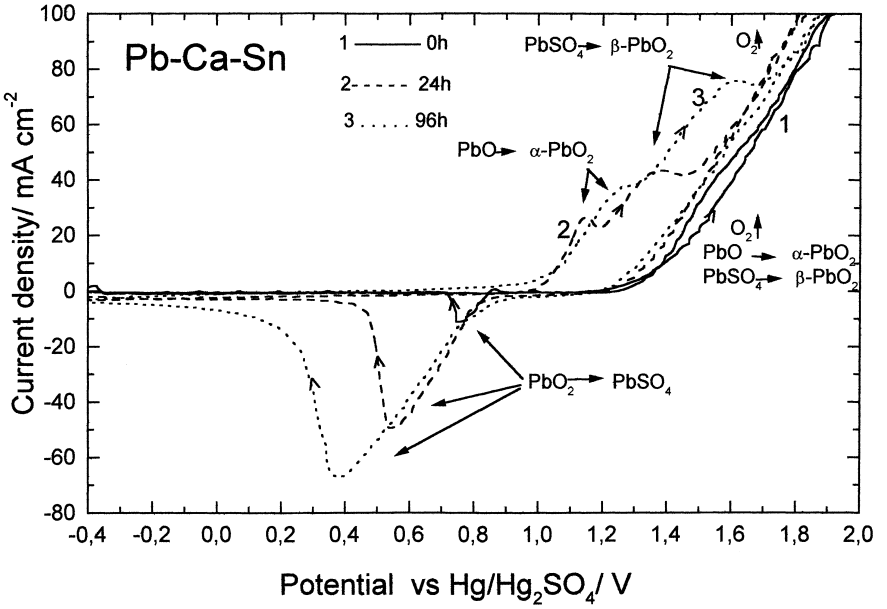

Fig. 2. Cyclic voltammograms of Pb–Ca–Sn anode obtained at the start time, at the 24th hour and at the 96th hour of the anodic polarization.

oxygen evolution is slightly shifted negatively. The well defined peaks of the oxidation of PbO to α-PbO_2 and of $PbSO_4$ to β-PbO_2 disappear; the anodic peak preceding the cathodic peak during scanning in the negative direction also disappears. The cathodic peak is shifted negatively (an increased height of the cathodic peak is also observed, hence the amount of PbO_2 formed on the surface increases during polarization). The shift of the anodic branch of oxygen evolution in a negative direction during polarization means that the oxygen evolution overpotential decreases. This effect is probably due to the continuous changes in phase composition (formation of $PbSO_4$, α-PbO_2, β-PbO_2 and other Pb compounds) [25]. It can be assumed that during prolonged electrowinning with a Pb–Sb anode, oxygen evolution is slightly depolarized and, moreover, the Pb–Sb anode becomes more prone to corrosion.

Figure 2 shows the cyclic voltammograms of the Pb–Ca–Sn anode at the start time, at the 24th hour and 96th hour of anodic polarization. The curve, corresponding to the start time is characterized by one anodic branch when scanning positively, and one anodic and one cathodic peak when scanning negatively. Similarly to the Pb–Sb anode, the sharp increase in anodic current begins at 1.45 V. The typical anodic peak, characterizing the formation of PbO_2 is not observed. It probably lies on the same place as the peak of oxygen evolution. The curves obtained at the 24th hour and 96th hour are characterized by two anodic peaks corresponding to an oxidation of PbO to α-PbO_2 and of $PbSO_4$ to β-PbO_2, by one anodic branch when scanning positively, and by one cathodic peak when scanning negatively. It may be suggested that, similarly to the Pb–Sb anode, oxygen evolution on the Pb–Ca–Sn anode is slightly depolarized in the course of time and the anode becomes more prone to corrosion.

Figure 3 shows the cyclic voltammograms of the composite Pb–Co_3O_4 anode at the start time, and after the 24th h and 96th hour of polarization. The curve corresponding to the start time is characterized by one anodic branch when scanning positively and one cathodic peak scanning negatively. The sharp increase in the anodic current begins at 1.2 V. Comparison with the corresponding curves of Pb–Sb and Pb–Ca–Sn anodes shows that oxygen evolution on Pb–Co_3O_4 is depolarized by nearly 0.25–0.3 V.

Figure 4 shows a SEM observation of a fresh Pb–Co_3O_4 anode. The white oval spots correspond to Co inclusions. It may be assumed that these sites act as active centres for oxygen evolution. The mechanism of Co action in oxygen evolution is described by Forsen et al. [14] who suggest that implantation of the Pb anode with Co or addition of Co^{2+} to the electrolyte leads to the formation of tetravalent CoO_2 and, in this case, oxygen subsequently evolves through decomposition of this unstable compound. The anodic peak, reflecting the

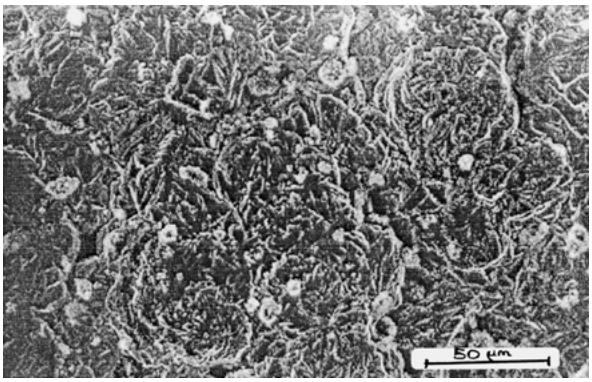

Fig. 4. Scanning electron micrograph of fresh Pb–Co_3O_4 anode.

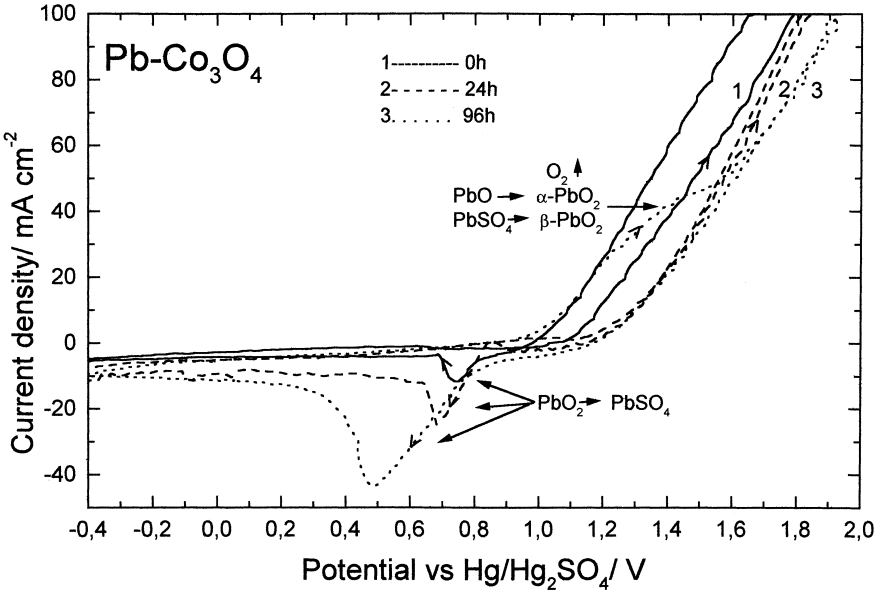

Fig. 3. Cyclic voltammograms of Pb–Co_3O_4 anode obtained at the start time, at the 24th hour and at the 96th hour of the anodic polarization.

formation of PbO_2 is not observed before 96 h. The CV curves in the potential range of oxygen evolution are shifted positively between the 0 and the 24th hour, and also between the 24th and the 96th hour, that is, the oxygen evolution reaction is polarized in the course of time. Probably, the surface layer formed on the composite Pb–Co_3O_4 coating becomes denser. It is clear, even without a microscope, that the composite Pb–Co_3O_4 coating has a highly spread active area. The formation of a surface layer on Pb–Co_3O_4 during prolonged polarization leads to a reduced active area of the anode as compared to the fresh anode (from 0 to 24 h). Similar changes in area of the surface layer are also observed during the 24th to 96th hours.

The height of the cathodic peaks increases with the time, and the peaks are shifted negatively. The formation of PbO_2 on the Pb–Co_3O_4 anode is inhibited and this effect is confirmed by the lower cathodic peak height during scanning negatively. The surface film on the Pb–Co_3O_4 anode likely contains a smaller amount of PbO_2. Comparison of the respective curves for the three anodes reveals that the height of the cathodic peak of the Pb–Co_3O_4 anode is approximately two times smaller than those of the cathodic peaks of Pb–Sb or Pb–Ca–Sn. Two conclusions may be based on the data above: the use of a Pb–Co_3O_4 anode in copper electrowinning leads to depolarization of the oxygen evolution reaction as compared to the case of Pb–Sb and Pb–Ca–Sn anodes, and on the other hand, this anode seems to be more corrosion resistant than Pb–Sb and Pb–Ca–Sn anodes. A similar inhibition effect on the formation of PbO_2, and a similar depolarizing effect on oxygen evolution have been observed both with Pb anode and Co^{2+} ions in the electrolyte in copper electrowinning [6], as well as with Pb–Co anode (obtained by the impulse technique) in zinc electrowinning [15].

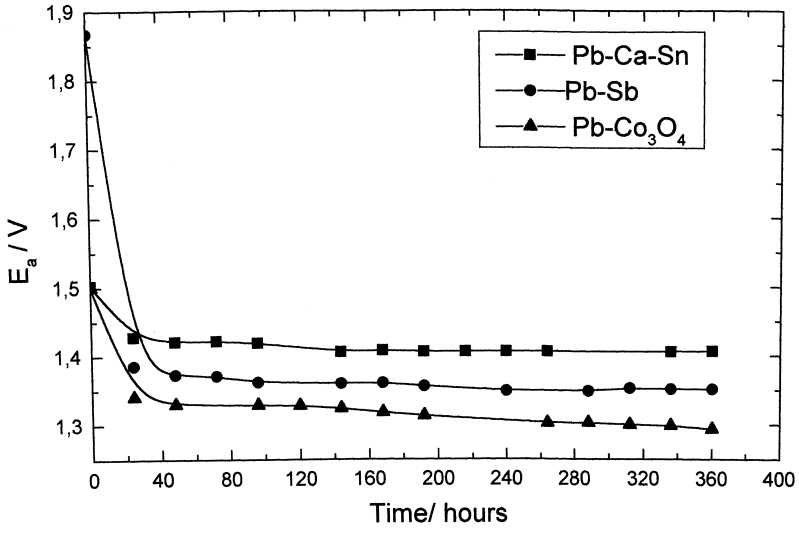

Fig. 5. Dependance of the anode potential (E_a) of Pb–Sb, Pb–Ca–Sn and Pb–Co_3O_4 anodes on time (h).

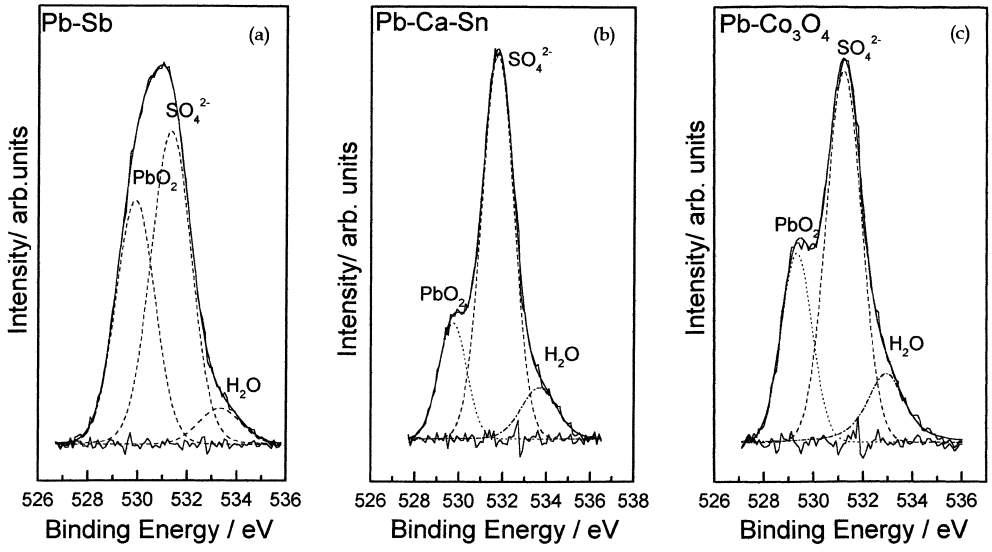

Fig. 6. XPS analyses of the anodic layer on Pb–Sb, Pb–Ca–Sn and Pb–Co_3O_4 anodes.

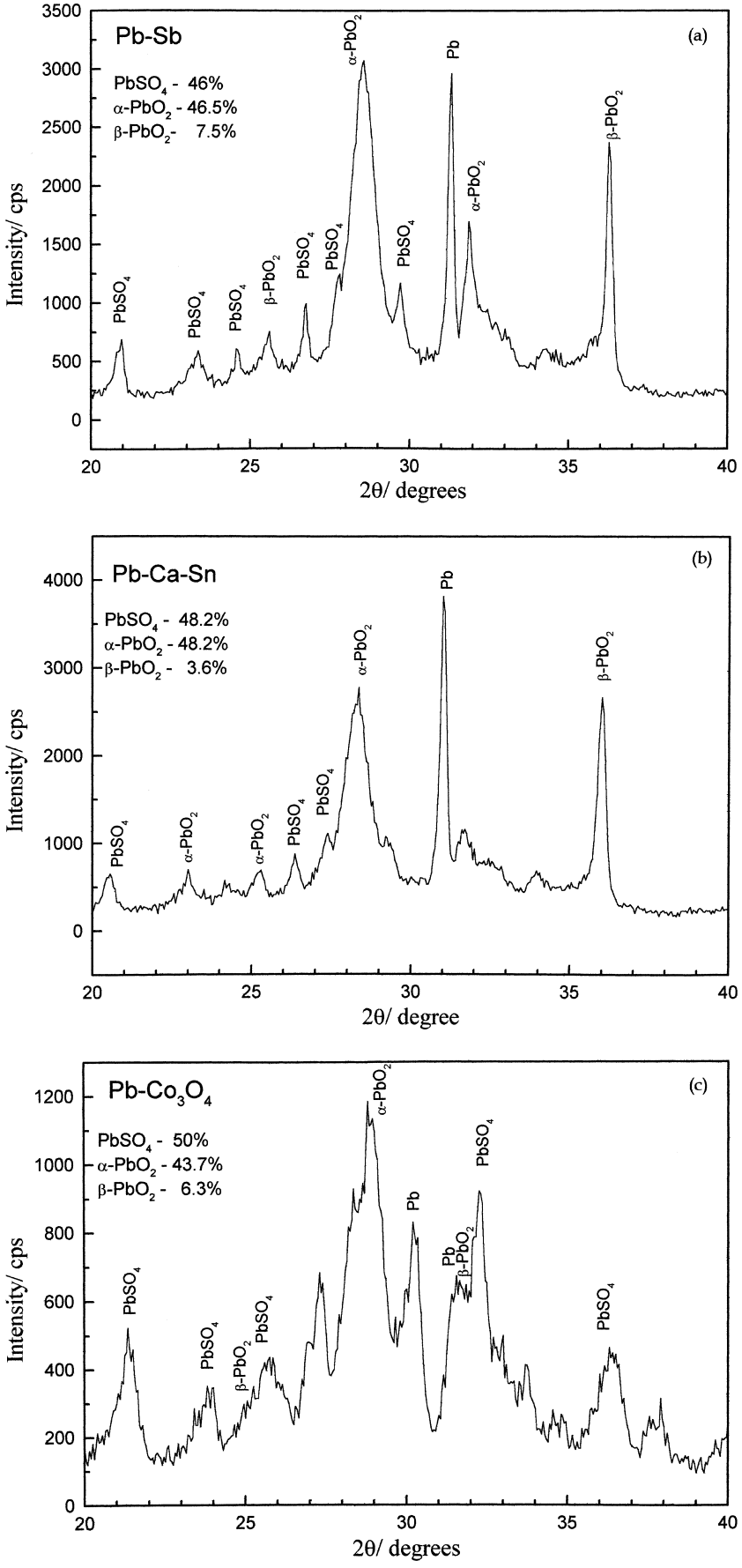

Fig. 7. X-ray analyses of the anodic layer on Pb–Sb, Pb–Ca–Sn and Pb–Co_3O_4 anodes.

3.2. *Anodic behaviour during prolonged electrolysis*

The Pb–Sb, Pb–Ca–Sn and Pb–Co_3O_4 anodes were subjected to potential–time measurements under galvanostatic conditions and the values of the anodic potential were registered every 24th hour during 360 h of polarization (Figure 5). The Pb–Ca–Sn and Pb–Co_3O_4 anodes show the same initial potential, while the initial potential of Pb–Sb anode is considerably higher. The anodic potential sharply decreases between the 0 and 24 h, when the anodic layer forms, and is almost unaltered after 24 h. The potential values of the Pb–Co_3O_4 anode are lower than those corresponding to Pb–Sb and Pb–Ca–Sn, which is an indication for the depolarizing effect of the Pb–Co_3O_4 anode on the anodic reaction. Some contradiction between the CV measurements and the galvanostatic investigations on the Pb–Co_3O_4 anode was evident. According to the CV curves, the oxygen overpotential increases in the course of polarization (96 h), while according to the galvanostatic curves there is an opposite trend (the oxygen overpotential decreases during polarization up to 360 h). This difference may be due to changes in active area of the anode surface layer. These are probably more pronounced at higher potentials during the scan (as explained in Section 3.1).

The corrosion resistance of the composite Pb–Co_3O_4 anode was evaluated approximately by measuring the concentration of Co^{2+} in the electrolyte, which is a result of Co_3O_4 dissolution during copper electrowinning. The Co^{2+} concentration was analysed by spectrophotometry. Co concentration in the electrolyte was lower than 0.01 mg l^{-1} after the 24, 48, 72 and 96 h.

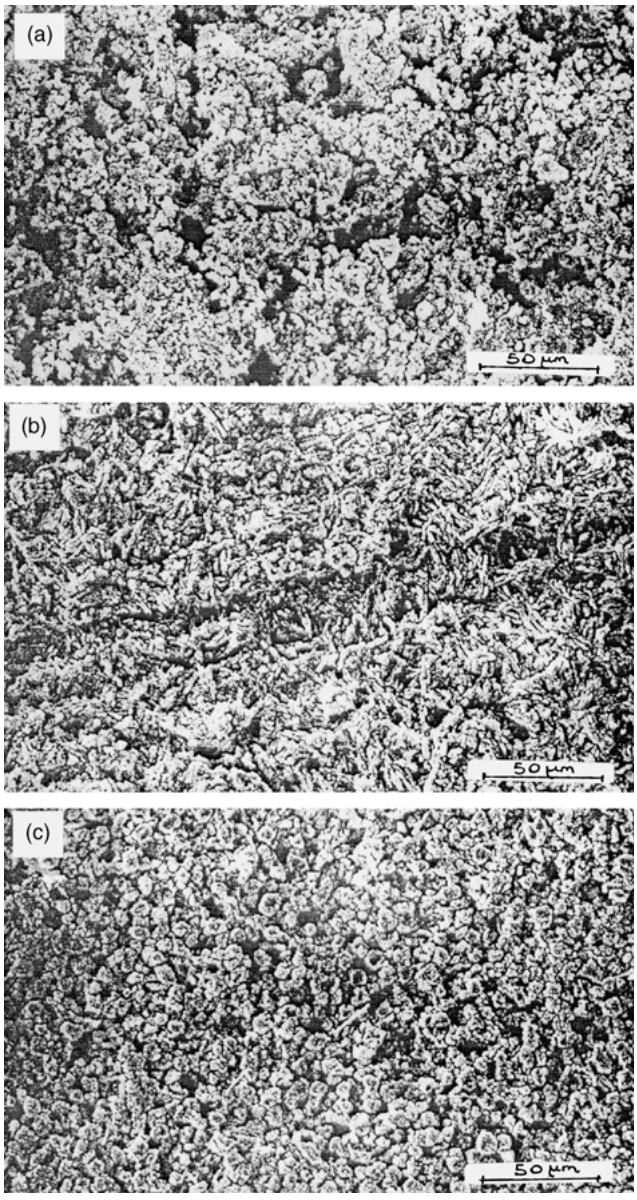

Fig. 8. Scanning electron micrographs (×500) of Pb–Sb (a), Pb–Ca–Sn (b) and Pb–Co_3O_4 anodes (c) at the 96th hour of polarization.

3.3. *Composition and structure of the anodic layer*

According to XPS data, the surface layer on Pb–Sb, Pb–Ca–Sn and Pb–Co_3O_4 mainly contains Pb^{2+} ($PbSO_4$) and Pb^{4+} (PbO_2) (Figure 6(a,b,c)). X-ray analysis has shown that the surface layer on Pb–Sb, Pb–Ca–Sn and on Pb–Co_3O_4 is mainly composed of α-PbO_2 and $PbSO_4$, and that it contains a small amount of β-PbO_2 (Figure 7(a,b,c)). The lowest amount of PbO_2 is found in the layer on the Pb–Co_3O_4 anode, hence in this case the process of $PbSO_4$ oxidation to PbO_2 is inhibited. (The amounts of α-PbO_2, β-PbO_2 and $PbSO_4$ are given in the corresponding X-ray photographs.)

Figure 8(a,b,c) shows SEM observations after 96 h of Pb–Sb, Pb–Ca–Sn and Pb–Co_3O_4 anodes, respectively. The surface film on Pb–Sb (Figure 8(a)) is loose and has a highly spread fine structure similar to a coral. Similar observations are reported with Pb [26] and Pb–Sb anodes [19]. The corresponding micrograph of Pb–Ca–Sn (Figure 8(b)) shows a fibrous structure. The micrograph of the Pb–Co_3O_4 anode (Figure 8(c)) indicates that the surface layer is dense, uniform and has a more fine-grained structure as compared to that on Pb–Sb and Pb–Ca–Sn.

4. Conclusion

During prolonged electrowinning under galvanostatic conditions, the anodic reaction on the Pb–Co_3O_4 anode is depolarized by 0.053 V as compared to the Pb–Sb anode, and by 0.106 V with respect to the Pb–Ca–Sn anode.

According to cyclic voltammetry, the formation of PbO_2 on the Pb–Co_3O_4 anode is inhibited, and according to X-ray spectra, the amount of PbO_2 on Pb–Co_3O_4 is smaller than on Pb–Sb and Pb–Ca–Sn. Therefore, a lower corrosion rate of the Pb–Co_3O_4 anode is expected.

Acknowledgements

The composite Pb–Co_3O_4 anode was developed at the Institute of Physical Chemistry, BAS, Bulgaria with the financial support of Union Miniere (UM) Company, Belgium. The authors are grateful to Dr R. Vermeersch from UM for his help and cooperation.

References

1. W.C. Cooper, *J. Appl. Electrochem.* **15** (1985) 789.
2. W. Hofman, 'Blei und bleilegirungen' (Springer Verlag, Berlin, 1962).
3. I.A. Aguf and M.A. Dosoian, *Vestnik Elektropromishlennosti* **10** (1959) 62.
4. A.S. Gendron, V.A. Ettel and S. Abe, *Canadian Metall. Quarterly* **14** (1975) 59.
5. G. Eggett and D. Naden, *Hydrometallurgy* **1** (1975) 123.
6. A.A. Kucherov, A.D. Artem'ev, N.A. Zaikova and V.N. Koganov, *Tsvetnie metali* **6** (1991) 25 (in Russian).
7. D.F.A. Koch, *Electrochim. Acta* **1** (1959) 32.
8. H. Borchers and H. Assmann, *Z. Metallkunde* **69** (1978) 43.
9. R.D. Prengaman, 7th International Lead Conference, Madrid (1980).
10. R.D. Prengaman, *in* D.J. Robinson and S.E. James (Eds), Proceeding of Sessions, 'Anodes for Electrowinning', AIME Annual Meeting, Los Angeles, CA (Feb. 1984), pp. 59–67.
11. R.D. Prengaman, *US Patent 4 376 093* (1983).
12. R.D. Prengaman, Proceedings of 44th Annual Meeting of IBMA, Chicago (1981).
13. T.U.D. Dunaev, 'Neraztvorimie anodi iz splavov na osnove svinca' (Nauka, Kazahskoi SSR, 1987), p. 209 (in Russian).
14. O. Forsen, J-J. Kukkonen, J. Aromaa and S. Ylasary, European Seminar 'Improved Technologies for the Rational Use of Energy in the Non-ferrous Industry in Europe' (Milan, Italy, 1992), pp. 127–138.
15. St. Rashkov, Ts. Dobrev, Z. Noncheva, Y. Stefanov, B. Rashkova and M. Petrova, *Hydrometallurgy* **52** (1999) 223.
16. M. Petrova, Y. Stefanov, Z. Noncheva, Ts. Dobrev and St. Rashkov, *Br. Corros. J.* **34** (1999) 198.
17. Y. Stefanov, M. Petrova, Z. Noncheva and Ts. Dobrev, *in* A. Topuz and N. Cansever (Eds), VIIth International Corrosion Symposium, Istanbul, Turkey (2000), pp. 63–70.
18. A. Hrussanova, L. Mirkova and Ts. Dobrev, *Hydrometallurgy* **60** (2001) 199.
19. B.K. Mahato, *J. Electrochem. Soc.* **126** (1979) 365.
20. M.P.J. Brennan, B.N. Stirrup and N.A Hampson, *J. Appl. Electrochem.* **4** (1974) 49.
21. Y. Yamamoto, K. Fumino, T. Ueda and M. Nambu, *Electrochim. Acta* **37** (1992) 199.
22. M. Skyllas Kazacos, *J. Electrochem. Soc.* **128** (1981) 817.
23. T. Laitinen, B. Monahov, K. Salmi and G. Sundholm, *Electrochim. Acta* **36** (1991) 953.
24. T.F. Sharpe, *J. Electrochem. Soc.* **122** (1975) 845.
25. D. Pavlov, Doctorate thesis, CLECPS-BAS (Central Laboratory of Electrochemical Power Sources), Sofia (1984).
26. A.C. Simon, S.M. Caulder and J.T. Stemmle, *J. Electrochem. Soc.* **122** (1975) 461.